Analysis of Spatial Pattern of Urban System along the Overland Silk Road Economic Belt Using DMSP-OLS Nighttime Light Data

Jianzhong Feng[a], **Linyan Bai**[b,*], **Kui wang**[b], **Xuefu Zhang**[a], **Nengfu Xie**[a], **Qiyun Ran**[b], **Mingqiu Guo**[b], **Lijun Xu**[c]
[a] Key Lab of Agri-information Service Technology, Ministry of Agriculture of P. R. China, Agricultural Information Institute, Chinese Academy of Agricultural Sciences, Beijing 100081, China;
[b] Institute of Remote Sensing and Digital Earth, Chinese Academy of Sciences, Beijing 100094, China;
[c] Institute of Agricultural Resources and Regional Planning, Chinese Academy of Agricultural Sciences, Beijing 100081, China.
Email: baily@radi.ac.cn

Abstract. As China promotes the Belt and Road (BAR) initiative, the overland SREB development is widely concerned. The cities (including towns), population centers, of urban system are the cores of the economy along the SREB. Therefore, it is necessary to monitoring the urbanization of the belt so that the new growing points of urban development and the valid coupling mechanism between human and nature will be explored to promote the regional socio-economic sustainable development and effectively implement the BAR initiative. Using the DMSP-OLS stable nighttime lights (NTL) data in 1992, 2003, and 2014, in this paper we studied the urbanized spatial patterns of and the urbanized characteristics and trends of the main city system along the SREB in the view of the whole regionalized economic zone and typical cities and settlements (towns). The results showed that in general the NTL intensities in the SREB's city system had the obvious geographical differentiation characteristics where there was maximum brightness of NTLs over the western European countries as well as being gradually decreasing from west to east. There were obvious increases of the NTL digital number (DN) values and NTL covering areas in 2003 and 2013 comparatively with that of 1992, which indicates the great urbanization development during this period. As for the four types of urban development process, there was an apparent consistency in a certain local area but a large heterogeneity among different areas. By analyzing the 273 pivot cities and the most pivot 26 cities, we found the number of the relatively small cities being decreasing but that of the large and medium-sized cities increasing. This study would provide the scientific support for the related researches and decision making of urbanization and urban economic development to promote the socio-economic comprehensive development of the overland SREB.

1. Introduction

As China promotes the Belt and Road (BAR), i.e., Silk Road Economic Belt (SREB) and 21st-Century Maritime Silk Road (21st-CMSR), initiative, the overland SREB development, which is a significant measure for mutually beneficial cooperation and common development among China and countries of central Asia and Europe, is widely concerned. It is also very important to expand and deepen the national strategy of China's Opening-up to the Outside World and brings to the corresponding provinces (such as Shaanxi, Gansu, and Xinjiang) along it opportunities of speeding up their social and economic development and promoting their deepening of reform (http://www.mofcom.gov.cn/article/resume/n/201504/20150400929655.shtml). The cities (including towns), population centers, of urban system are the cores of the economy along the SREB, which crucially support and drive its socio-economic development. Therefore, it is necessary to monitoring the urbanization of the belt (such as urban development situation, urbanization mode and trend so that the new growing points of urban development and the valid coupling mechanism between human and nature will be explored to promote the regional socio-economic sustainable development and effectively implement the BAR initiative.

The Operational Linescan System (OLS), which can detect light emission from the earth surface at night, is carried on a series of satellites of the US Air Force (USAF) Defense Meteorological Satellite Program (DMSP). The DMSP-OLS has a ground swath of about 3000 km. It has two broad

spectral bands, one covering the visible-near infrared region (0.4 - 1 μm) and the other is in the thermal infrared region (10 - 13 μm). The OLS data are acquired in two spatial resolution modes: 'fine' and 'smoothed'. The full resolution fine data have a nominal spatial resolution of 0.56 km. On board averaging of five by five blocks of fine data produces "smoothed" data with a nominal spatial resolution of 2.7 km. The DMSP-OLS has a ground swath of about 3000 km. It has two broad spectral bands, one covering the visible-near infrared region (0.5 - 0.9 μm) and the other is in the thermal infrared region around 10 μm. The OLS data are acquired in two spatial resolution modes: 'fine' and 'smoothed'. The full resolution fine data have a nominal spatial resolution of 0.56 km. On board averaging of five by five blocks of fine data produces "smoothed" data with a nominal spatial resolution of 2.7 km. Most of the data received by NOAA-NGDC is in the smoothed spatial resolution mode (http://www.crisp.nus. edu.sg/~research/tutorial /dmsp.htm) (Liao et al., 2012). The DMSP-OLS has a unique capability to observe faint sources of visible-near infrared emissions present at night on the Earth's surface, including cities, towns, villages, gas flares, heavily lit fishing boats and fires (Chen et al., 2003; & Wang et al., 2012). By analyzing a time series of DMDP-OLS images, it is possible to define a reference set of "stable" lights, which are present in the same location on a consistent basis, and easily explore the significant human activities such as characterization of urban extent and spatial change. Specifically, there are caveats inherent to the fact that the area and intensity of illumination (detected by the DMDP-OLS) are known to vary significantly with energy availability, economic development and density of settlement (Elvidge et al., 1997; Sutton et al, 1997; Small et al., 2005; Elvidge et al., 1999; Hao et al., 2014). At present, the digital data from DMDP-OLS (since 1992) can provide three products of stable, radiance calibrated, and non-radiance calibrated nighttime lights (Hao et al., 2014; Ziskin et al., 2010; Elvidge et al., 2001).

Using the DMDP-OLS stable nighttime lights data in 1992, 2003, and 2014, in this paper we studied the urbanized spatial patterns of and the urbanized characteristics and trends of the main urban system along the SREB.

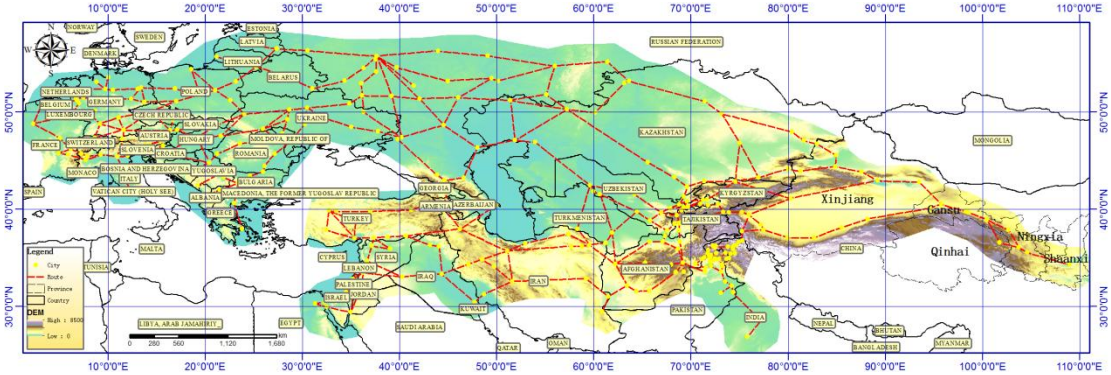

Figure 1. The landscape of the Overland Silk Road Economic Belt and pivot cities

2. Data and methods

2.1 Data and processing correction for imagery

DMSP-OLS stable nighttime light data (coving cities, townships, and other lasting light emissions), background noise of which has been removed, are derived from National Oceanic and Atmospheric Administration's (NOAA's) National Geographic Data Center (NGDC), and the grey value of data ranges from 0 to 63, meaning that value 0 represents the unlit area and the greater the grey value, the higher the light level of the region will be (Wu et al, 2013). Now the products of 34 satellite years (Version 4) derived from six satellites (F10, F12, F14, F15, F16, and F18) from 1992 to 2013 are available for downloading from NGDC (http://www.ngdc.noaa.gov /dmsp/download.html). In this study we used the stable light data, which have the same reference ellipsoid as the World Geodetic System 1984 (WGS-84), derived from the satellites, i.e., F10 (1992), F14 and F15 (2003), and F18 (2013), where nighttime passes of the DMSP typically occurred between 20:30 and 21:30 local time (Elvidge et al, 2001; Yang et al., 2011). The spatial resolution of data is 30 arc-seconds, about one kilometer from the equator, spanning -180 ° to 180 ° longitude and -65 ° to 75 ° latitude, which represents the basic global coverage of human activity areas, and then the data were transformed into the Lambert azimuthal equal-area

projection so as to accurately represent area in all regions of the sphere and define the extent of interest areas. Given the fact that the continuity and comparability of images derived from the DMSP different satellites are often lacking, e.g., the amounts and geographical locations of lots of pixels in the same annual light images of different sensors are inconsistent with each other and/or the pixels' digital number (DN) values are very different (Zou et al., 2014), we employed a linear regression model to empirically fix the stable light data for 1992-2003 and 2003-2013 respectively, as shows:

$$DN_{fixing}(year) = \alpha(year \parallel average\_year) \cdot DN_{original}(year) + \varepsilon_{year} \qquad (1)$$

where DN_{fixing} is a correct value of each pixel, and α is a correction coefficient, and *year* is 1992 and 2013, and *average_year* is a benchmark year of 2003, and $DN_{original}$ is a original value of corresponding pixel, and ε is a constant term.

Owing to obviously stable nighttime lights in different annual images, their corresponding pixels can easily be probed through valid spatial features. Based on the DN average values of each pixel of two chose stable nighttime light images (from F14 and F15) in 2003, we used a moving window with 8×8 pixels to detect the matching spatial textures of the light data for 1992 and 2013, respectively, in order to obtain the available pixels for training the above correction formula (1). There are two achieved correction coefficients of $\alpha(1992 \parallel 2003)$ = 0.980 with ε_{1992} = 0.255 (R^2 = 0.953, n = 6358) and $\alpha(2013 \parallel 2003)$ = 1.008 with ε_{2013} = 0.737 (R^2 = 0.981, n = 8121) (see Table 2), which means their own fine fitting relationships greatly valid for correction of the light data, respectively.

The high-resolution dataset of country administrative areas, derived from the Database of Global Administrative Areas (downloaded from URL of http://www.gadm.org on March-30-2016), with a few export formats of shapefiles used in most common Geographic Information System (GIS) applications, were utilized to overlap on the corrected nighttime light data, and the main cities and towns along the Silk Road Economic Belt (SREB) were selected from high-definition (see Figure 1), high-resolution imagery (e.g., Google Earth imagery with Version V7.1.2.2041, 2013) and located to the light data. Based on the broken linking line of the chose cities and towns, a set-on-demand buffer with different diameters was produced in terms of its local actual situation by using the ArcGIS software, and the study zone (region) of the SREB was thus obtained.

Additionally, The land cover data was derived from the annual GlobCover 2009 land cover product with the full resolution of 300m, produced by the European Space Agency (ESA) in collaboration with its partners (i.e., EEA, FAO, GOFC-GOLD, IGBP, JRC and UNEP) (downloaded from the website of http://www.esa.int/due/ionia/globcover). The global land cover product was produced from an automatic and regionally-tuned classification of a time series of global Medium Resolution Imaging Spectrometer Instrument (MERIS on board the ENVISAT satellite mission) Fine Resolution (FR) for the year 2009, which counts 22 land cover classes defined with the United Nations (UN) Land Cover Classification System (LCCS), i.e., croplands, forests, shrubland, grassland, artificial surfaces and associated areas (including urban areas), bare areas, water bodies, and permanent snow and ice, etc. The Digital Elevation Model (DEM) dataset was derived from the NASA/USGS Shuttle Radar Topography Mission (SRTM) 90m resolution digital elevation database with the geographic coordinate system of WGS84 (Version 4.1) (downloaded from the website of http://srtm.csi.cgiar.org /SELECTION/inputCoord.asp or http://srtm.datamirror. csdb.cn/search.jsp, i.e., http://www.gscloud.cn/), offered by the Consortium for Spatial Information (CGIAR-CSI) of the Consultative Group for International Agricultural Research (CGIAR). The GlobCover 2009 land cover and SRTM 90m DEM data are used to analyze the study area's urban spatial dynamics and development trend of urbanization synthetically associated with the previous DMSP nighttime light data (Li et al., 2007).

2.2 Extracting urban spatial scopes

Urban spatial area size, shape, and distribution are the basic elements to study urban types, spatial pattern, and population, etc.. It was necessary to extract the spatial scopes of urban cities and large settlements along the SREB, and we chose key 322 cities and towns (settlements) in the economic zone, where being a principle to choose traffic hubs, i.e., indicative population, supplies and goods distribution centers, and typically examined them to further understand the spatial pattern and urbanization of this city system. Based on the DMSP-OLS stable lights data, a spatial contrast method was used to determine the optimal group of a minimum marginal digital number value (which initially defined a urban space) and dynamical match a DN threshold so as to exactly detect urban local areas, which was iterated to extract the spatial scopes of urban cores, and it has a significantly easy, effective advantage with a high accuracy (Mi et al., 2013). Then, in this study region the spatial pattern of urban system were analyzed and the urban expansion mode, velocity, and trend were discussed with the urbanization process of the SREB by using urban land-cover spatial indices such as land cover diversity, area shape, fragmentation, and compactness parameters (Wang et al., 2006; Ma & He, 2008; Li & Yang, 2012).

2.3 Urbanized spatial intensity and pattern transition exploration for urban system

Given that urban land is a base of urban social and economic development, the reasonably intensive land development is known as a basic tactics to save land resource. Thus, urban central areas often have a high level of spatial accumulation, which indicates their intensity and concentration, and corresponding land uses while peripheral areas have lower levels of accumulation. Urbanized (land use) spatial intensity (USI) is commonly defined with a intensive degree of land use and/or land cover per unit urban area, which is measured by population density, invested capital density of urban land, or energy consumption per unit area, etc. (Yue, 2002).The urban stable night-light intensity can generally well represent utilization intensity of urbanized (land use) space because of their strong correlation (Elvidge et al. 2001; Amaral et al. 2006). Using the DMSP-OLS stable night-light data as proxy data of urbanized spatial intensity (USI), we are able to readily probe the general utilization efficiencies of urban land-use/cover spaces, spatial pattern and variation characteristics, and their spatially collaborative coupling relationships through the urban night-light intensity monitoring and analyses. These are very significant to understand and predict the changes of urbanized spatial pattern (e.g., conversion of parcel land use and extension of urban areas) and urbanization process laws, etc. and promote the urban ecological security and urban socio-economic sustainable development along the SREB.

Obviously, spatial pattern of urbanized (land use) spatial intensities, as shown at the city level or at the regional city group level, is essentially the comprehensive mapping of regional economic, social, and ecological structures, that is, the orderly combination conformation of the quantity structure and spatial forms of urbanized spatial intensity index within a scope of regionalized urban space, and the change of the fore can often inevitably lead to the correspondence of the latter and vice versa; meanwhile, spatial changes of urban land use make the quantity structure and spatial forms of urbanized spatial intensities present specific spatial and temporal evolution characteristics and laws in regional areas of a city or city and town system.

We chose the DMSP-OLS stable nighttime light data in 1992, 2003, and 2013 as proxy data sources of urbanized spatial intensity to explore the spatial-temporal development characteristics of urban land use/cover for the SREB's urban system in nearly 20 years. In order to efficiently reveal the gradually gradient development tendency of spatial pattern of urbanized spatial intensity (or, urban land cover) in this study area, a false color composite (FCC) image was created based upon three bands of Red (R), green (G), and blue (B) orderly assigned to the time series NTL data, respectively, where being stretched for color composition, as shows:

$$MONO\_DN_{color(i)} = \alpha/\beta \times DN(i) \qquad (2)$$

where $MONO\_DN_{color(i)}$ is a color component of each pixel of the false color image at color(i) = R, G or B band, and $\alpha+1 = 256$ and $\beta+1 = 64$ are the color grey-scale number and rank number of NTL data, respectively, and

DN represents the DN value of each pixel of NTL images in i = 1992, 2003, and 2014.

There is an evident merit as to each urban pixel (or potential urban pixel) of the false color image that apparently displays the dynamic situation of its urbanized spatial intensity and corresponding spatial combination (or accumulation) characteristics of pixels, i.e., urbanized spatial pattern gradient changes in nearly 20 years for the SREB's city system, so it effectively transforms the contents of static night-light panel data of different periods into a visual process array with intuitive spatial segregation information. The subtle changes at the pixel level are thus easily identified as well as it avoids that error accumulation caused by urbanized spatial intensity classification results in reducing detection accuracy of land use/cover changes. As shown in table 1, there are 8 types of dynamic modes of pixels for urbanized spatial intensity along the SREB during nearly two decade period, and we can lightly identify the urbanized spatial intensity changes, urban spatial development types and trends: for example, the urbanized spatial intensities of urban land use and cover in type 1-6 areas were increasing, which indicate that the areas are emerging urban plats, but the type 7 and 8 areas are recessing urban places because their corresponding urbanized spatial intensities were decreasing.

ID	Condition	Express	Meaning
1	A≥0, b≥0 & c≥1	E-E-A	Expansion during 1992-2003, and a accelerated expansion during 2003-2013
2	A≥0, b≥0 & c＜1	E-E-S	Expansion during 1992-2003, and a slow expansion during 2003-2013
3	A≥0, b＜0 & c≥1	E-S-A	Shrinkage during 1992-2003, and a accelerated expansion during 2003-2013
4	A≥0, b＜0 & c＜1	E-S-S	Shrinkage during 1992-2003, and a slow expansion during 2003-2013
5	A＜0, b≥0 & c≥1	S-E-A	Expansion during 1992-2003, and a accelerated shrinkage during 2003-2013
6	A＜0, b≥0 & c＜1	S-E-S	Expansion during 1992-2003, and a slow shrinkage during 2003-2013
7	A＜0, b＜0 & c≥1	S-S-A	Shrinkage during 1992-2003, and a accelerated shrinkage during 2003-2013
8	A＜0, b＜0 & c＜1	S-S-S	Shrinkage during 1992-2003, and a slow shrinkage during 2003-2013

*Note: $a = DN_{2013} - DN_{2003}$; $b = DN_{2003} - DN_{1992}$; $c = \left|\frac{a}{b}\right|$, and Expanding: E; Shrinking: S; A: Accelerating.

Table 1. Gradient development modes of urbanized spatial pattern

Year	Function construction			Validation		
	Pixels	Function	R^2	Pixels	r^2, P	F, t Test
1992	6358	$DN'_{1992}=0.255+0.980\times DN_{1992}$	0.953	1281	R^2=0.93, P<0.001	F=18132.08, T=7.50
2013	8121	$DN'_{2013}=0.737+1.008\times DN_{2013}$	0.981	1497	R^2=0.92, P<0.001	F=17717.53, T=7.85

Note: where R^2 and r^2 are the fitting, testing coefficients of determination, respectively, and P for the significant levels.

Table 2. Construction and validation of the Modify function

3. Results and discussion

3.1 Overall existing situation and trends of the SREB's urbanization development

We employed the 4 nighttime light (NTL) images from 4 satellites, F10 (1992), F14 and F15 (2003), and F18, and then, using the corresponding linear regression models that were relied on a stable light detection algorithm with a texture detector of a moving window with 8 × 8 pixels (see Section 2), the bi-temporal images (1992 and 2013) were corrected to reduce the system errors of NTL data, which were caused by the different performances of the satellite sensors, based upon the average value of two images in 2003 as a benchmark. As shown in Table 2, there are good consistencies between the correct and benchmark data.

The three temporal revised NTL data (in 1992, 2003, and 2013) were utilized to extract the urban spatial areas

of the cities and towns along the Silk Road Economic Belt (SREB) by using a spatial contrast method at the pixel level (Mi et al., 2013) (see Figure 2) and farther explore the urbanized expansion. Meanwhile, the NTL intensities in the three images served as the proxy of urbanized (land use/cover) spatial intensities to detect their spatial characteristics and dynamic trends. In general, the NTL intensities in the SREB's city system had the obvious geographical differentiation characteristics where there was maximum brightness of NTLs over the western European countries as well as being gradually decreasing from west to east, but the NTLs over a small area of the southeast (namely, in parts of India) always had relatively high brightness during this period of years. Contrasted on that of 1992, there is an apparent increase of pixels with lower non-zero DN values in the image of 2003, suggesting that a large number of small towns (settlements) may be emerging until the time, whereas the NTL intensities remain about the same or increase slightly over the large and medium cities of Central Asia, which means a low speed urbanized expansion over the cities. However, the number of light pixels and their light brightness in the image of 2013 all have obviously increased, comparing with that of 2003, meaning there was a rapid urbanized expansion in this study region. We aimed at the 273 pivot cities from the chose 322 cities and towns, and summed up their urban spatial areas and DN values of NTL intensities (namely, urbanized spatial intensities) in 1992, 2003, and 2013, respectively, in order to further analyze the urbanized development (urban sprawl or urban decay) of the SREB's city (and towns) system. Although the total urban spatial area and total urbanized spatial intensity value in 2003 increase about 15.87% and 16.33% respectively in the case of that of 1992, there are obviously greater corresponding increases (about 66.13% and 75.28%, respectively) about that of 2013 and 2003 (see Table 3), which indicates faster urbanized expansion and regionalized economic development speeds during 1992-2003 that of 2003-2013, that is to say, we reached the same conclusion with what's mentioned above.

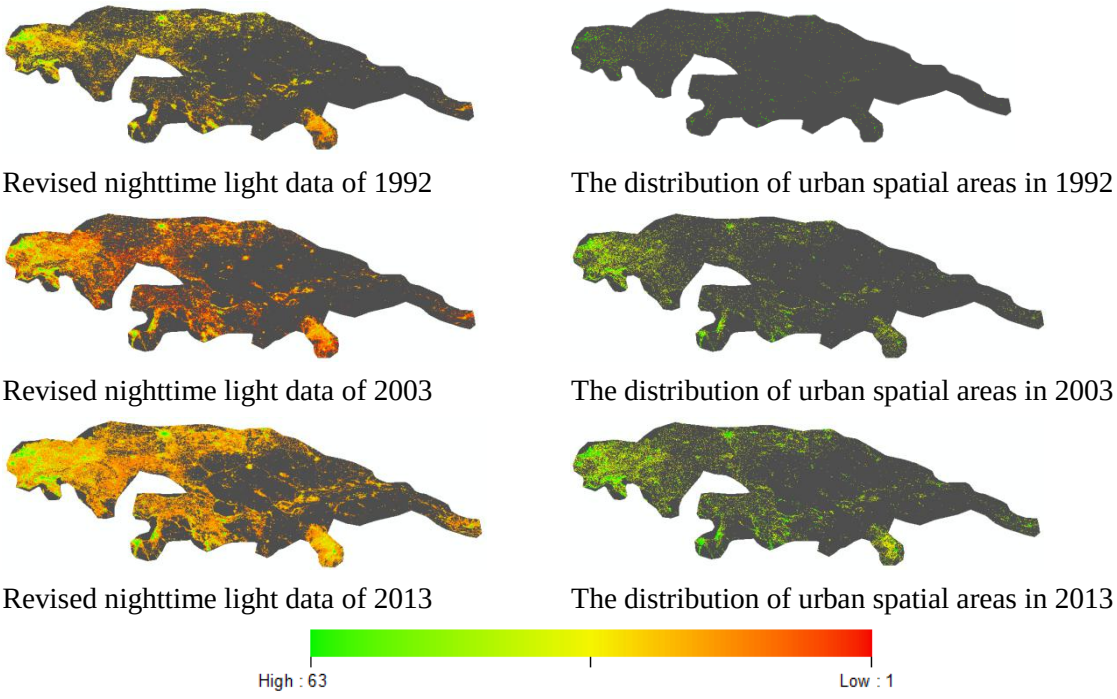

Figure 2. The three temporal revised nighttime light data and the distribution of urban spatial areas of the cities and towns in 1992, 2003, and 2013 along the Silk Road Economic Belt

				1992 to 2003		2003 to 2013	
1992	2003	2013		increased value	Growth ratio	increased value	Growth ratio

DN	37491 13	43614 32	76448 06	9	61231	0.1633	328337 4	0.7528
Areas (km2)	39195	45416	75450		6221	0.1587	30034	0.6613

Table 3. The statistic characteristics of area and sum of DN with the cities in 1992, 2003 and 2013

3.2 Urbanized spatial pattern and gradient characteristics along the SREB

In order to efficiently reveal the gradually gradient development tendency of spatial pattern of urbanized spatial intensity (or, urban land cover) in this study area, a false color composite (FCC) image was created based upon three bands of Red (R), green (G), and blue (B) orderly assigned to the time series NTL data (i.e., in 1992, 2003, and, 2013), respectively, which were used as proxy data sources of urbanized spatial intensities. Due to the close correlation between the urban NTL intensity and the associated urbanized spatial intensity and level of urban economic development, the trend of the NTL intensity change represents the corresponding urban development process. As shown in Figure 3(a), the red areas, which display scattered distribution mainly in the past Soviet Union (now parts of Russia and Ukraine, etc.), indicate that NTL maximum brightness values appeared in 1992, meaning their corresponding urbanized spatial intensities (or economic development situations) may present continuous falter and underperform after 1992. The green areas appeared in 2003, located mainly in the urban areas of Central and Eastern Europe, urbanized spatial intensities of which could increase first and then fall off. The blue areas, being scarce and mainly in small parts of Russia and India, appeared in 2013, which presented fast growth during 2003-2013, and the white indicates developed areas that are huge metropolises (such as Moscow and Delhi) and the vast Western Europe. The yellow areas presented more bright lights in 1992 and 2003, but the light intensities somewhat decreased until 2013, which means their urbanized spatial intensities increasing during 1992-2003 and to a certain declining during 2003-2013. The purple areas showed more bright lights in 1992 and 2013, but being weaker in 2003, economies of which represented being recession first and then growing. The blue-green were due to more bright lights in 2003 and 2013 but being weaker in 1992, urbanized spatial intensities of which had continued growth first with a high speed and then somewhat were slowing sales growth.

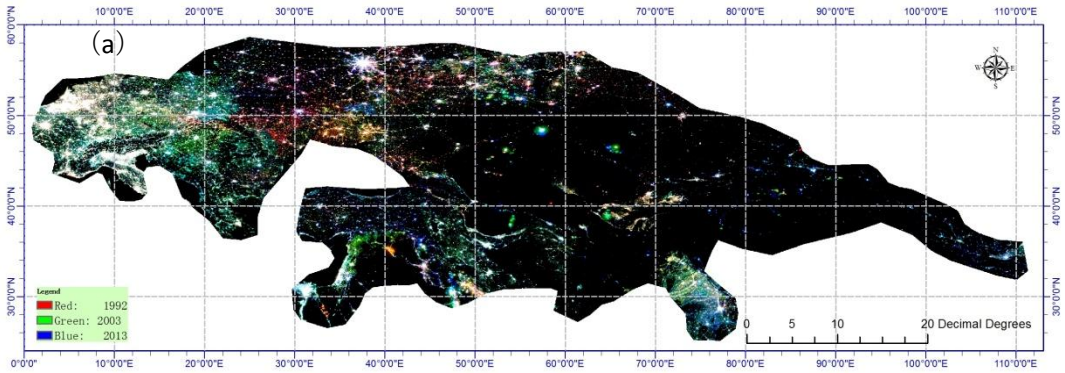

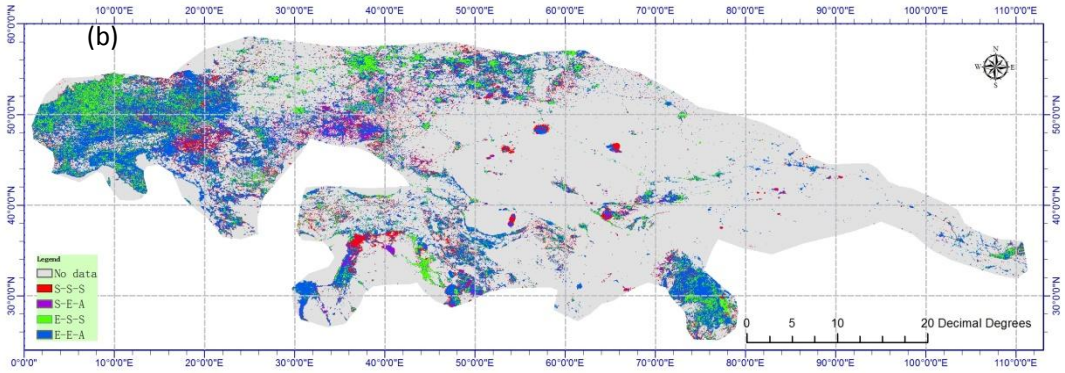

Figure 3. Nighttime light composites. (a) is represented by a primary colour (R:1992/G:2003/B:2013). (b) is Urbanized gradient mode distribution along the Silk Road Economic Belt

Hereon, according to the multiple gradient development modes of urbanized spatial pattern (see Table 1), we used the NTL data in 1992, 2003, 2013 to produce an urbanized spatial gradient mode image (see Figure 3(b)) so as to further identify the changes of NTL intensities, analyze and understand the urbanized spatial patterns and regional urban economic development and trends in this study area. There are four types of S-S-S, S-E-A, E-S-S, and E-E-A where S, E, and A correspondingly represent shrinking, expanding, and accelerating, respectively. It is obvious that the blue areas are the largest scope which indicates their on-going economic growth in faster speeds, and the green areas are located in the Moscow region of Russia and the northwest of Europe, etc., which suggest recession during 1992-2003 but slow growth after 2003. The small red and purple areas lie mainly in the urban areas of Eastern Europe and parts of the Middle East, and the Southern Ukraine, respectively.

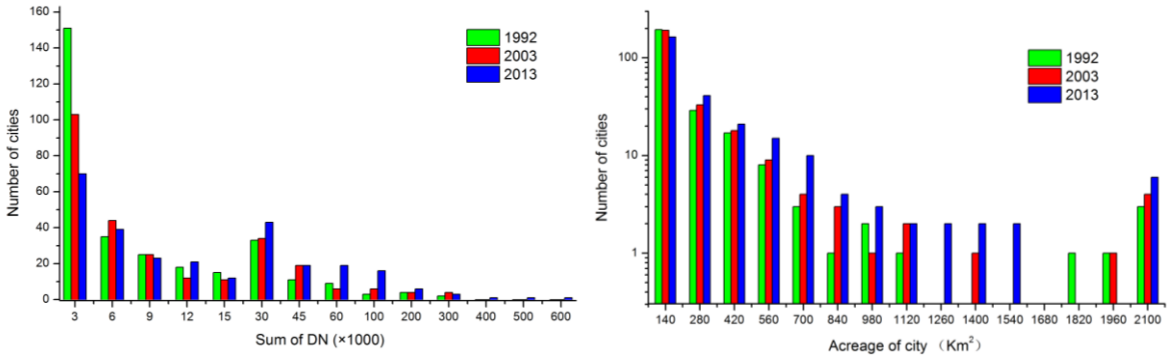

Figure 4. The frequency of the sum of DN value and acreage of 273 pivot cities

Name	Shape index			Fragmentation			Compactness		
	1992	2003	2013	1992	2003	2013	1992	2003	2013
Almaty	0.90	0.67	0.46	0.08	0.02	0.01	0.33	0.38	0.42
Amsterdam	0.64	0.48	0.35	0.03	0.01	0.00	0.25	0.30	0.37
Astana	1.27	0.91	0.48	0.10	0.02	0.02	0.37	0.39	0.39
Paris	0.27	0.24	0.21	0.01	0.01	0.00	0.28	0.32	0.34
Berlin	0.31	0.34	0.30	0.01	0.01	0.00	0.46	0.45	0.46
Bishkek	0.92	0.58	0.45	0.07	0.02	0.01	0.46	0.76	0.67
Brussel	0.49	0.43	0.31	0.02	0.01	0.00	0.32	0.37	0.44
Tehran	0.58	0.52	0.44	0.04	0.02	0.01	0.15	0.15	0.14
Dushanbe	0.51	0.69	0.54	0.01	0.02	0.01	0.46	0.71	0.68
Warszawa	0.79	0.73	0.42	0.04	0.04	0.01	0.21	0.22	0.31
Kyiv	0.45	0.46	0.27	0.01	0.01	0.00	0.47	0.51	0.64
Kabul	0.90	1.54	0.49	0.07	0.13	0.01	0.59	0.47	0.55
Kashi	2.06	1.22	0.81	0.35	0.08	0.02	0.58	0.48	0.47

Lanzhou	1.06	0.72	0.51	0.03	0.02	0.01	0.34	0.39	0.43
Lyon	0.72	0.52	0.41	0.04	0.01	0.00	0.23	0.28	0.32
Rotterdam	0.36	0.34	0.23	0.01	0.00	0.00	0.32	0.34	0.45
Mashhad	0.77	0.71	0.72	0.05	0.03	0.03	0.25	0.25	0.19
Milano	0.57	0.32	0.17	0.02	0.01	0.00	0.14	0.22	0.38
Moskva	0.52	0.46	0.17	0.02	0.01	0.00	0.15	0.18	0.33
Samarqand	0.58	0.63	0.60	0.02	0.02	0.02	0.76	0.77	0.77
Venezia	1.05	0.56	0.20	0.07	0.01	0.00	0.16	0.23	0.48
Urumchi	1.39	0.64	0.29	0.11	0.02	0.00	0.25	0.41	0.54
Xi'an	1.13	0.84	0.42	0.09	0.06	0.02	0.18	0.19	0.22
Islamabad	0.83	0.63	0.41	0.06	0.04	0.01	0.34	0.39	0.41
Yining	0.00	0.00	0.48	0.00	0.00	0.01	0.00	0.00	0.81
Duisburg	0.00	0.46	0.39	0.00	0.01	0.01	0.00	0.63	0.67

Table 4. Shape index, fragmentation, compactness of special pivot cities in 1992, 2003, 2013

In order to deeply understand the urbanization process of the SREB's city system in nearly 20 years, we chose the specially pivot cities and analyzed their landscape indices, i.e., Shape Index, Fragmentation, and Compactness. From table 4, we could find that in general the big cities often have their own low Shape Indices and Compactness degrees, compared with that of small and medium-sized cities, but there are no significant differences in terms of Fragmentation degrees. These may result from the fact that with their urbanization development, the core areas of a big city were gradually joining with the surrounding satellite cities, which leads to their Shape Indices and Fragmentation degrees declining but their Compactness degrees increasing.

4. Conclusion

We employed the 4 NTL images from 4 satellites, F10 (1992), F14 and F15 (2003), and F18, and then, using the corresponding linear regression models that were relied on a stable light detection algorithm with a texture detector of a moving window, the bi-temporal images (1992 and 2013) were corrected to reduce the system errors of NTL data, based upon the average value of two images in 2003 as a benchmark. The revised NTL data were utilized to extract the urban spatial areas of the cities and towns along the Silk Road Economic Belt (SREB) by using a spatial contrast method at the pixel level, and Meanwhile the NTL intensities in the three images served as the proxy of urbanized (land use/cover) spatial intensities, in order to detect their spatial characteristics and dynamic trends. In order to efficiently reveal the gradually gradient development tendency of spatial pattern of urbanized spatial intensity in this study area, a false color composite (FCC) image was created based upon three bands of Red (R), green (G), and blue (B) orderly assigned to the time series NTL data respectively, which were used as proxy data sources of urbanized spatial intensities. According to the multiple gradient development modes of urbanized spatial pattern, we used the NTL data in 1992, 2003, 2013 to produce an urbanized spatial gradient mode image and further identify the changes of NTL intensities, analyze and understand the urbanized spatial patterns and regional urban economic development and trends in this study area.

In this paper, we studied the urbanized spatial patterns of and the urbanized characteristics and trends of the main city system along the SREB in the view of the whole regionalized economic zone and typical cities and settlements (towns). The results showed that in general the NTL intensities in the SREB's city system had the obvious geographical differentiation characteristics where there was maximum brightness of NTLs over the western European countries as well as being gradually decreasing from west to east. There were obvious increases of the NTL DN values and NTL covering areas in 2003 and 2013 comparatively with that of 1992, which indicates the great urbanization development during this period. As for the four types of urban development process, there was an apparent consistency in a certain local area but a large heterogeneity among different areas. By analyzing the 273 pivot cities and the most pivot 26 cities, we found the number of the

relatively small cities being decreasing but that of the large and medium-sized cities increasing. This study would provide the scientific support for the related researches and decision making of urbanization and urban economic development to promote the socio-economic comprehensive development of the overland SREB.

Acknowledgements

The work was supported by the Natural Science Foundation of China (NSFC) under Grant Nos. 41171340 and 41101390. This study was also supported by the Major International Cooperation and Exchange Project of National NSFC (Grant No. 41120114001), the Western Light Talent Culture Project (YBXM-2014-05), and the Science and Technology Innovation Program (for Agricultural Information Institute) of Chinese Academy of Agricultural Sciences (2016).

References

Amaral, S., A. M. V. Monteiro, A. M. V., Camara, G. & Quintanilha, J. A., 2006. DMSP/OLS night-time light imagery for urban population estimates in the Brazilian Amazon. International Journal of Remote Sensing, 27, pp. 855–870.

Chen, J., Zhuo, L. & Shi, P. J., et al., 2003. The study on urbanization process in china based on DMSP/OLS data: development of a light index for urbanization level estimation. Journal of Remote Sensing, 7, pp. 168-175.

Elvidge, C. D., Baugh K. E. & Dietz J. B., et al., 1999. Radiance calibration of DMSP-OLS low-light imaging data of human settlements. Remote Sensing of Environment, 68, pp. 77-88

Elvidge, C. D., Baugh, K. E., Kihn, E. A., Kroehl, H. W., Davis, E. R., & Davis, C. W., 1997. Relation between satellite observed visible–near infrared emissions, population, economic activity and electric power consumption. International Journal of Remote Sensing, 18, pp. 1373-1379.

Elvidge, C. D., Imhoff, M. L. & Baugh K. E., et al., 2001. Night-time lights of the world: 1994-1995. ISPRS Journal of Photogrammetry and Remote Sensing, 56, pp. 81-99.

Hao, R. F., Yu, D. Y., Liu, Y. P. & Sun, Y., 2014. Use of DMSP/OLS nighttime light data in urbanization monitor. Journal of Beijing Normal University (Natural Science), 50, pp. 407-413.

Li, J. G., He, C. Y., Shi, P. J. & Chen, J., et al., 2007. The Use of multisource satellite and geospatial data to study the ecological effects of urbanization: a case of the urban agglomerations in Bohai Rim. Journal of Remote Sensing, 11, pp. 115-126.

Li., C. Y & Yang, M., 2012. Quantity and spatial structure analysis of land resources in Xishan area of taiyuan city. Journal of Anhui Agri. Sci., 40, pp. 11088-11089, 11107.

Liao, B., Wei, K. X. & Song, W. W., 2012. Assessment and application of DMSP/OLS nighttime light data in the spatial structure of urban system: a case of Jiangxi province in nearly 16 years. Resources and Environment in the Yangtze Basin, 21, pp. 1295-1300.

Ma, Y. X. & He., B., 2008. Quantitative and spatial structure analyse for land use in Taiyuan city. J. Shanxi Agric. Univ. (Natural Science Edition), 28, pp. 121-124.

Mi, X. N., Bai, L. Y., Tan, X. H. & Lu., N., et al., 2013. A new method of extracing areas of center city regions based on DMSP/OLS data. Journal of Geo-information Science, 15, pp. 255-261, 279.

Small, C.; Pozzi, F. & Elvidge, C. D., 2005. Spatial analysis of global urban extent from DMSP-OLS night lights. Remote Sensing of Environment, 96, pp. 277-291.

Sutton, P., Roberts, C., Elvidge, C., & Meij, H., 1997. A comparison of nighttime satellite imagery and population density for the continental united states. Photogrammetric Engineering and Remote Sensing, 63, pp. 1303-1313.

Wang, H., Zheng, X. Q. & Yuan, T., 2012. Overview of researches based on DMSP/OLS nighttime light data. Progress in Geography, 31, pp. 11-18.

Wang., Z. L., Yang., Q. Y., Lu., C. Y. & Zhang, Z., D., 2007. Analysis on spatial structure of land

utilization in Shapingba district of Chongqing city. Resources & Industries, 9, pp. 90-93.

Wu, J. S., He, S. B., Peng, J. & Li, W. F., et al., 2013. Intercalibration of DMSP-OLS night-time light data by the invariant region method. International Journal of Remote Sensing, 34, pp. 7356–7368.

Yang, Y., He, C. Y., Zhao, Y. Y. & Li, T., et al., 2011. Research on the layered threshold method for extracting urban land using the DMSP/OLS stable nighttime light data. Journal of Image and Graphics, 16, pp. 666-673.

Yue, J. F., 2002. Real estate law dictionary. The Post & Telecom Press, in Beijing.

Ziskin, D., Baugh, K. & Hsu, F. C., et al., 2010. Methods used for the 2006 radiance lights. Proceedings of the 30th Asia-Pacific Advanced Network Meeting, pp. 131-142.

Zou, J. G., Chen, Y. H., Tian, J. & Wang T., 2014. Construction of the calibration model for DMSP/OLS nighttime light Images based on ArcGIS. Journal of Geomatics, 39, pp. 33-37.